Research Square

Preprints are preliminary reports that have not undergone peer review.
They should not be considered conclusive, used to inform clinical practice,
or referenced by the media as validated information.

Characterisation of Spatial Variability of Lacustrine Clay via Penetrometer Tests: A Case Study from Southern Brazil

André Luis Meier

de.luis.meier@gmail.com

Universidade Federal de Santa Catarina

Gracieli Dienstmann

Universidade Federal de Santa Catarina

Mariana Alher Fernandes

Universidade Federal de Santa Catarina

Jonatas Sosnoski

Universidade do Estado de Santa Catarina

Article

Keywords: spatial variability, lacustrine clay, penetrometer tests, scale of fluctuation, random field theory, full-flow penetrometers

Posted Date: August 10th, 2026

DOI: https://doi.org/10.21203/rs.3.rs-10509438/v1

License: This work is licensed under a Creative Commons Attribution 4.0 International License.
Read Full License

Additional Declarations: No competing interests reported.

Characterisation of Spatial Variability of Lacustrine Clay via Penetrometer Tests: A Case Study from Southern Brazil

André Luis Meier[a]*, Gracieli Dienstmann[a], Mariana Alher Fernandes[ab] and Jonatas Sosnoski[c]

[a]*Postgraduate Program in Civil Engineering, Federal University of Santa Catarina, Florianópolis, Brazil*

[b]*Department of Civil Engineering, Federal University of Technology – Paraná, Apucarana, Brazil*

[c]*Department of Civil Engineering, State University of Santa Catarina, Joinville, Brazil*

Corresponding author:

André Luis Meier (de.luis.meier@gmail.com)

+55 (47) 99633-2645

Word count (main text): 4393

Characterisation of Spatial Variability of Lacustrine Clay via Penetrometer Tests: A Case Study from Southern Brazil

This paper investigates the spatial variability of a soft lacustrine clay deposit in Tubarão, southern Brazil, via piezocone (CPTu), piezoball, and piezo-T full-flow penetrometer tests. Vertical scales of fluctuation (δ_v) and inherent variability coefficients (COV_w) were derived from seven in situ soundings at two adjacent sites. The random field theory framework was applied, incorporating stationarity verification via Kendall's tau test and fitting four theoretical autocorrelation models (SNX, SQX, CSX, SMK). The single exponential model provided the best fit for most profiles, with δ_v values ranging from 0.12 to 0.43 m for penetration resistance, with is consistent with typical ranges reported for marine and lacustrine clays worldwide. The full-flow penetrometers exhibited lower penetration resistance than did the piezocone but yielded consistent undrained shear strength estimates after site-specific bearing capacity factors were applied (N_{kt} = 15.5, N_b = 13.0, N_t = 11.8). Probability density function analysis revealed that the Weibull distribution best represented the grouped datasets. The findings confirm the applicability of full-flow penetrometers for spatial variability characterisation of soft clay deposits and provide useful statistical parameters for reliability-based geotechnical design, reinforcing the importance of careful preprocessing and model selection in random field analyses.

Keywords: spatial variability; lacustrine clay; penetrometer tests; scale of fluctuation; random field theory; full-flow penetrometers

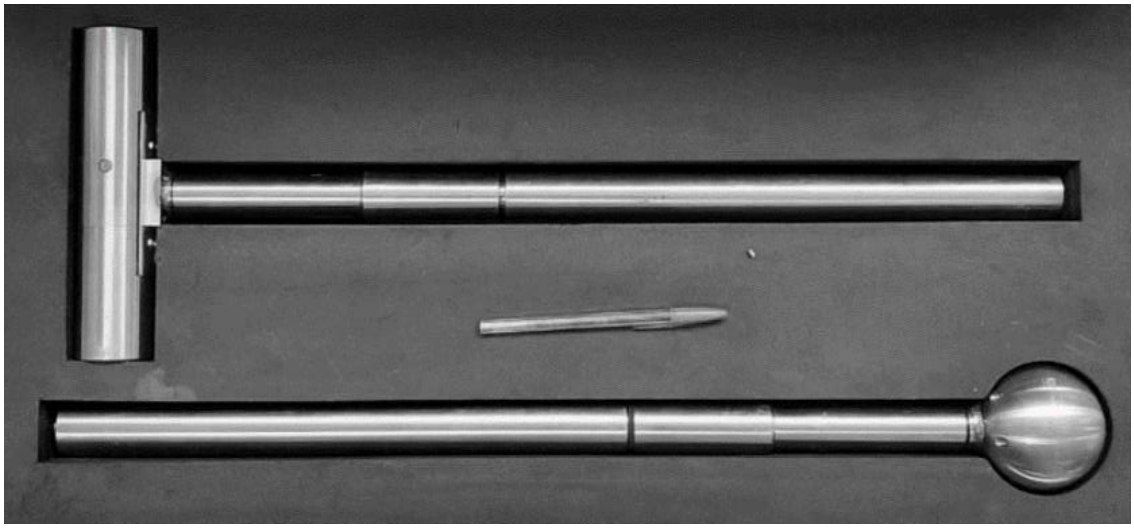
Introduction

Inherent soil variability represents a form of aleatory uncertainty, arising from the geological processes responsible for the formation and evolution of soil deposits [1]. In geotechnical engineering, spatial variability is commonly described via random field theory, wherein uncertainty is characterised by the mean, standard deviation, and scale of fluctuation [2]. This characteristic can be quantified through laboratory testing and in situ investigation methods, which provide the necessary data to define the statistical distribution and spatial variability of soil properties.

The piezocone penetration test (CPTu) is one of the most widely used in situ tests for identifying subsurface profiles and determining spatial variability, owing to its continuous data acquisition capability [3]. This equipment enables the estimation of soil properties from measurements of cone tip resistance (q_c), sleeve friction (f_s), and pore pressure (u), providing continuous profile interpretations and derivations of key geotechnical design parameters such as undrained shear strength (S_u). Cone penetration resistance is influenced by multiple soil characteristics, including stiffness, stress state, strength anisotropy, and drainage conditions during penetration [4, 5, 6, 7, 8]. In this sense, accurate estimation of the undrained shear strength of soft soil deposits remains challenging, often because of the selection of an appropriate cone bearing capacity factor (N_{kt}), which depends on site-specific soil characteristics [9, 10].

To address these limitations, in situ full-flow penetrometers, such as piezoball and piezo-T (Figure 1), were developed to improve characterisation of soil resistance compared with conventional CPTu. These devices induce a full-flow mechanism around the probe owing to their spherical or cylindrical geometries [11]. When the full-flow regime is reached the measured penetration resistance exhibits reduced sensitivity to soil characteristics, requiring only minor corrections for overburden stress and pore pressure [9, 12, 13]. In such cases, bearing capacity factors, designated N_b for the piezoball and N_t for the piezo-T, are still needed to interpret the penetration resistance. Nevertheless, the available literature indicates that these factors generally exhibit a narrower range of variation than the N_{kt} factor commonly adopted for CPTu interpretation does, which may contribute to improving the reliability of undrained shear strength estimates [14].

Figure 1.



Coastal zones frequently contain soft soil layers resulting from sedimentary geological processes, particularly marine deposits. In these environments, piezocone and field vane shear tests (FVTs) are the predominant investigation methods, although full-flow penetrometers, such as piezoball and piezo-T, have received increasing attention in recent years because of their potential to improve the estimation of undrained shear strength in very soft soils [e.g., 15, 16].

Numerous studies have investigated the spatial variability of soft clay deposits via CPT/CPTu data within the framework of random field theory. These investigations cover a wide range of geological settings, including Australia [17], Italy [18], the United States [19, 20, 21], Norway [22], China [2, 23], Tanzania [24], Singapore [25], and Korea [26]. However, to the authors' knowledge, no previous studies have explored the use of piezoball or piezo-T data for the characterization of spatial variability, which represents a key contribution of the present study.

A further important consideration of spatial variability analysis is the rigorous preprocessing of sounding profiles before estimating statistical parameters. Random field modelling assumes that soil properties can be represented as the combination of a

deterministic trend and a stationary random residual component [1, 27]. Consequently, profile segmentation, detrending, and verification of stationarity are essential steps for obtaining reliable estimates of spatial variability parameters. Studies, such as that of Lim and Lee [26], have quantified the influence of different trend functions, as well as the number of lags and expressions considered for estimating the scale of fluctuation, thereby contributing to a more rational and systematic treatment of spatial variability data. Integrated approaches incorporating machine learning (ML) techniques for profile segmentation have also been reported in the literature, as described by Macedo et al. [28]. Nevertheless, despite these advances, the characterization of soil variability across material transitions, such as clay–sand interfaces, remains a significant challenge and is not always consistently addressed in practice.

In this context, to contribute both to the broader application of full-flow penetrometers and to their use for estimating statistical descriptors of soil variability, the present study performs a rigorous assessment through a direct quantitative comparison between the spatial variability descriptors obtained from conventional piezocone (CPTu) tests and those derived from piezoball and piezo-T tests. The study is based on a database comprising piezocone, piezoball, and piezo-T flow penetrometer tests conducted on a soft clay deposit in Tubarão, southern Brazil. The dataset, compiled following the frameworks established by Meert [29] and Sosnoski [30], includes seven soundings. Spatial variability parameters derived from piezoball and piezo-T tests are evaluated and compared with those obtained from conventional piezocone tests. Particular emphasis is given to the determination of key random field parameters, including the vertical scale of fluctuation (δ_v), following rigorous trend removal and verification of data stationarity. The inherent variability of the undrained shear strength (S_u) is subsequently investigated for geotechnical design purposes through the evaluation of theoretical probability density

functions (PDFs), together with the determination of the mean values and coefficients of variation (COVs) for each test type. The results provide the first assessment of the applicability of full-flow penetrometers for spatial variability characterization in Brazilian soft clays and contribute to the selection of random field parameters for reliability-based geotechnical analyses.

Theoretical Background

Random field modelling

The inherent spatial variability of soil deposits results from natural geological formations and postdepositional processes, which continuously modify the soil mass in situ [1]. This variability, along with measurement and transformation uncertainties, is a major source of uncertainty in geotechnical analysis. Its proper characterisation is essential for reliability-based design and probabilistic assessments [31].

Random field theory (RFT) provides a probabilistic framework for describing the correlation structure of soil properties [32]. Under RFT, a spatially varying property $g(z)$ at depth z can be decomposed into a deterministic trend $t(z)$ and a fluctuating (residual) component $w(z)$:

$$g(z) = t(z) + w(z) \quad (1)$$

The trend represents large-scale variations (e.g., an increase in penetration resistance with effective stress), whereas the fluctuating component captures small-scale inherent variability [17, 33]. The residual $w(z)$ is typically modelled as a stationary random field characterised by three parameters: the mean μ, standard deviation σ (or coefficient of variation, COV), and scale of fluctuation δ [32].

The scale of fluctuation (δ), also called correlation length, measures the distance over which soil properties remain strongly correlated [1]. A large δ indicates smooth, highly correlated variations; a small δ implies rapid, short-range fluctuations [34]

A prerequisite for applying RFT is weak stationarity: a constant mean and autocovariance depend only on the lag distance [35]. For a weakly stationary field, δ is defined as twice the area under the positive part of the autocorrelation function [27, 32]:

$$\delta = \int_{-\infty}^{+\infty} \rho(\tau) d\tau = 2 \int_{0}^{+\infty} \rho(\tau) d\tau \quad (2)$$

where $\rho(\tau)$ is the autocorrelation function and τ is the lag distance.

To achieve stationarity, the deterministic trend $t(z)$ must be removed, leaving the residual $w(z)$. In this study, stationarity was verified via Kendall's tau test at 95% confidence [36].

Autocorrelation Function Approach

The autocorrelation function (ACF) approach is widely used to estimate the scale of fluctuation from in situ test data [34, 37; 38]. It involves two main steps: (i) computing the sample autocorrelation function (SAF) from the detrended data and (ii) fitting theoretical autocorrelation models (TAMs) to the SAF.

The sample autocorrelation coefficient $\rho(\tau_j)$ for lag $\tau_j = j\,\Delta z$ (where Δz is the sampling interval and j is the lag number) is calculated as [17, 34]:

$$\rho(\tau_j) = \frac{\sum_{i=1}^{n-j}(x_i - \mu_x)(x_{i+j} - \mu_x)}{\sum_{i=1}^{n}(x_i - \mu_x)^2} \quad (3)$$

where n is the number of data points, x_i is the property value at depth z_i, and μ_x is the mean. The lag distance is as follows:

158 $$\tau_j = (j-1)\cdot \Delta z \quad (4)$$

159 The theoretical autocorrelation models used in this study are summarised in Table
160 1 (see Methods for fitting details).

161 Table 1. Theoretical autocorrelation models and corresponding scale of fluctuation [34].

Model	**ACF**	**δ**
SNX	$\rho(\tau) = e^{-2\left\|\frac{\tau}{\delta}\right\|}$	$\delta = \frac{2}{k}$
SQX	$\rho(\tau) = e^{-\pi\left\|\frac{\tau}{\delta}\right\|^2}$	$\delta = \frac{\sqrt{\pi}}{k}$
CSX	$\rho(\tau) = e^{-\left\|\frac{\tau}{\delta}\right\|} \cdot \cos\left(\left\|\frac{\tau}{\delta}\right\|\right)$	$\delta = \frac{1}{k}$
SMK	$\rho(\tau) = e^{-4\left\|\frac{\tau}{\delta}\right\|} \cdot \left(1 + 4\left\|\frac{\tau}{\delta}\right\|\right)$	$\delta = \frac{4}{k}$

162

163 Additionally, stationary random fields can be classified as isotropic when the
164 scale of fluctuation is independent of direction, or anisotropic, when different scales of
165 fluctuation are required to represent the spatial structure of the material. Anisotropic
166 models are generally more appropriate for sedimentary deposits, where depositional
167 processes promote the formation of horizontally stratified soil layers, leading to different
168 spatial correlation lengths in the vertical and horizontal directions (δ_v and δ_h,
169 respectively). In the present study, only the vertical variability is investigated; therefore,
170 the analyses are restricted to the characterisation of the vertical scale of fluctuation
171 ($\delta = \delta_v$).

Methods

Field Testing Procedures

The investigation campaigns were conducted in accordance with national and international technical standards. Piezocone tests from both campaigns were executed according to ASTM D5778 [39] and NBR 12069 [40], with a standard penetration rate of 20 mm/s. For the full-flow penetrometer tests, the same hydraulic pushing system was employed, with a penetration rate of 20 mm/s in accordance with the recommendations of ISO 19901-8 [41]. Slight procedural variations were observed between the two campaigns. In Meert [29], piezoball tests (MB1, MB2) were advanced to a depth of -13.0 m, with dissipation tests conducted at four distinct depths (-2.8 m, -4.8 m, -6.8 m, and -8.8 m), during which pore pressure measurements were recorded at the tip (u_1), mid-face (u_2), and equator (u_3) positions. In Sosnoski [30], piezoball tests (SB1, SB2) were performed to depths of -10.2 m (SB1) and -11.0 m (SB2), with dissipation tests carried out at four distinct depths (-4.0 m, -6.0 m, -8.0 m, and -10.0 m). The piezo-T test was performed only in Sosnoski [30] and advanced to a depth of -11.0 m at a constant rate of 20 mm/s; however, no pore pressure records were obtained because of transducer malfunctions. The variations in execution procedures were related primarily to the determination of remoulded strengths, which are beyond the scope of the present study and therefore will not be further discussed.

Data processing and stationarity verification

The raw sounding data were processed following the steps described below. For each test, the soil behaviour type index $I_{C,RW}$ was evaluated at every measurement point [42]. On the basis of the $I_{C,RW}$ profiles, one or more homogeneous layers were identified for each sounding. A linear polynomial trend was then removed, and the stationarity of the

196 residuals was verified via Kendall's tau test at 95% confidence [36]. For cone tip
197 resistance (q_c for piezocone, q_m for full-flow), if the residuals failed the test, localised
198 outliers or spikes were removed and the procedure was repeated until passing. Once
199 the q_c(or q_m) profiles were stationary, the remaining parameters, sleeve friction f_s, pore
200 pressures u_2 (and u_1, u_3 for piezoball), and undrained shear strength S_u, were evaluated
201 without further data removal, as the layer definition was already established. Note
202 that S_u is derived directly from q_c and q_m using bearing capacity factors (N_{kt}, N_b, N_t);
203 therefore, removing a linear trend preserves the same correlation structure for S_u.
204 To characterise the remaining scatter of the detrended profiles, the inherent
205 coefficient of variation (COV_w) was calculated for each parameter. COV_w reflects the
206 variability of the residual $w(z)$ after trend removal, independent of depth-dependent
207 trends [1, 34]. The statistical significance of the detrending procedure was assessed via
208 Kendall's tau test; all p-values > 0.05 indicate stationarity at 95% confidence.

209 ***Spatial Variability and Autocorrelation Modelling***
210 To ensure reliable estimates of the scale of fluctuation (δ), the maximum number of lags
211 (m) employed in the computation of the sample autocorrelation function must be
212 appropriately constrained. Several criteria for selecting m are available in the literature.
213 These encompass fixed empirical bounds, such as $m = 12$ [43] or $20 \leq m \leq 40$ [44,
214 45], as well as formulations dependent on the total number of data points (n),
215 including $m = n/4$ [36, 46, 47] and $m = \sqrt{n} + 10$ [48]. Additionally, Bartlett's limit,
216 defined as $m = 1.96/\sqrt{n}$ [28, 34, 49], provides a statistical upper bound for reliable
217 autocorrelation estimates. Davis [50] noted that estimation accuracy improves
218 when n exceeds 50.

In the present study, three criteria were evaluated to ensure robustness against sensitivity to the chosen maximum lag: (i) $m = 12$ [43]; (ii) $m = \sqrt{n} + 10$, which yielded values between 20 and 40 for the dataset analysed [44, 45, 48]; and (iii) $m = n/4$, the most commonly adopted criterion in geotechnical studies [36, 46]. The adoption of multiple criteria is intended to provide a comprehensive assessment of the correlation structure and to minimise potential biases associated with a single arbitrary choice of m.

After the SAF was obtained, four TAMs were fitted via least-squares regression: single exponential (SNX), squared exponential (SQX), cosine exponential (CSX), and second-order Markov (SMK) [34, 39]. Their functional forms and δ relationships are given in Table 1. The best TAM was selected on the basis of the coefficient of determination R^2, with values above 0.9 indicating a good fit [35].

The trend removal procedure followed the steps described in the previous subsection [28, 35, 36]. This approach was sufficient to achieve weak stationarity for the lacustrine clay, as verified by Kendall's tau test at 95% confidence for all the profiles analysed.

Probabilistic distribution fitting

In addition to the spatial correlation structure, the inherent variability of the grouped data was characterised by fitting probability distributions to the measured parameters, as described below. Four probability distributions – normal, lognormal, gamma, and Weibull – were evaluated to represent the grouped data. The goodness-of-fit was assessed through histogram analysis, Q–Q plots, and quantitative error metrics derived directly from comparisons between theoretical and empirical quantiles. Specifically, the Pearson correlation coefficient (R) and the root mean square error (RMSE) were calculated from the Q–Q plot data, providing objective measures of the agreement between the theoretical

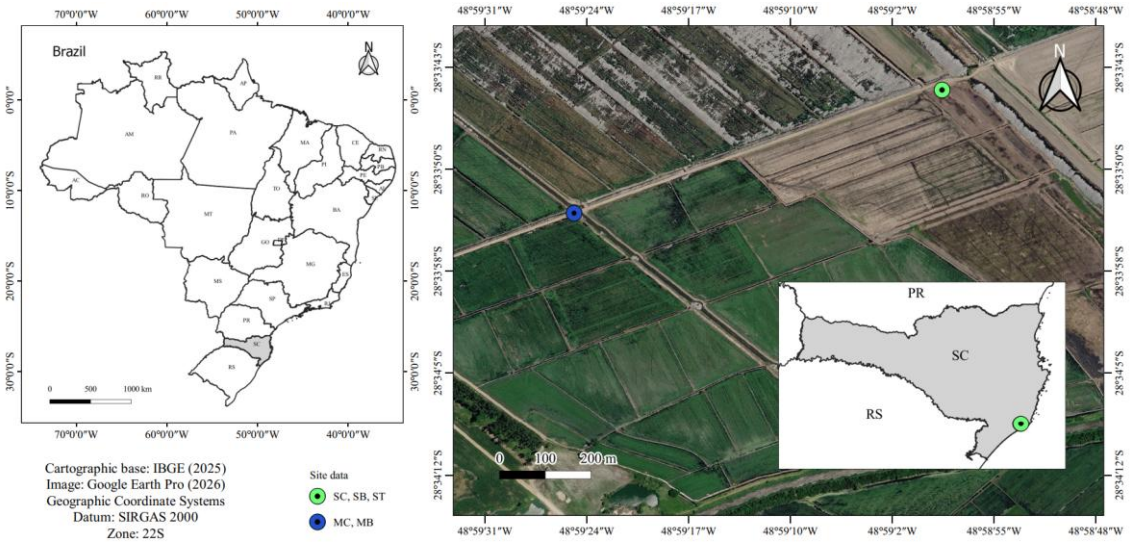
distributions and the observed dataset.

Site description

The study site is located within the Tubarão River Delta, southern Brazil. The region is bounded to the north and west by the Precambrian crystalline basement of the Atlantic Shield, and to the south and east by lacustrine and aeolian depositional systems [30, 51, 52].

The local stratigraphy comprises a Quaternary sedimentary deposit, with upper Holocene layers approximately 20 m thick. These deposits formed soft soils, normally consolidated to lightly overconsolidated, with high water content, elevated organic matter, high compressibility, and low shear strength [53]. The spatial distribution of the geotechnical investigation campaigns at the Tubarão Testing Site is shown in Figure 2.

Figure 2.

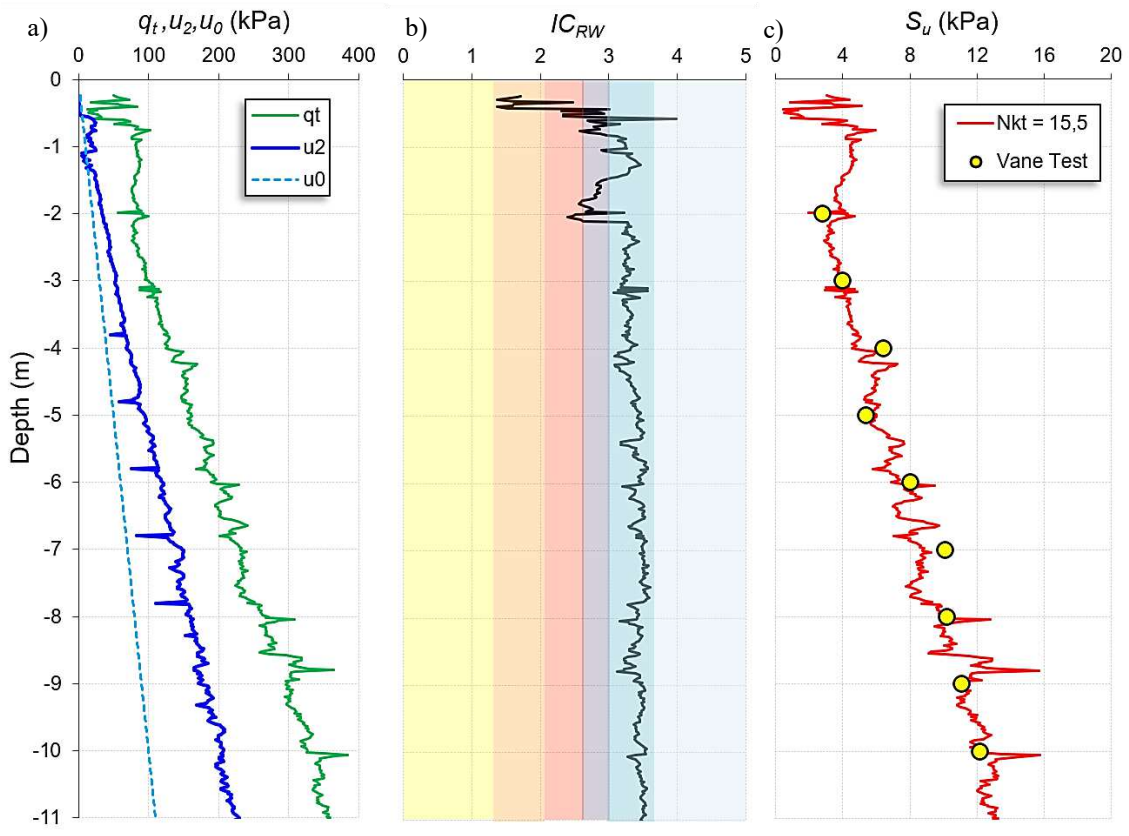


Previous studies have characterised the Tubarão region via piezocone tests, vane tests, Marchetti dilatometer tests, and laboratory tests [29, 30, 53, 54, 55]. For this

research, we used the databases from Meert [29] and Sosnoski [30], which include piezocone, piezoball, and piezo-T flow penetrometer tests.

A representative stratigraphic profile (Figure 3), which is based on piezocone data from Sosnoski [30], shows a clay layer from near the surface down to 11.0 m, with corrected cone resistance q_t ranging from 100 to 400 kPa (Figure 3a). Significant excess pore pressure u_2 is observed throughout the depth. The soil behavior index $I_{C,RW}$ [42] indicates that the deposit is primarily clay (Figure 3b). The undrained shear strength S_u profile was established via a calibrated bearing capacity cone factor $N_{kt} = 15.5$, which agrees well with the vane shear test data (ranging from 3–12 kPa, Figure 3c).

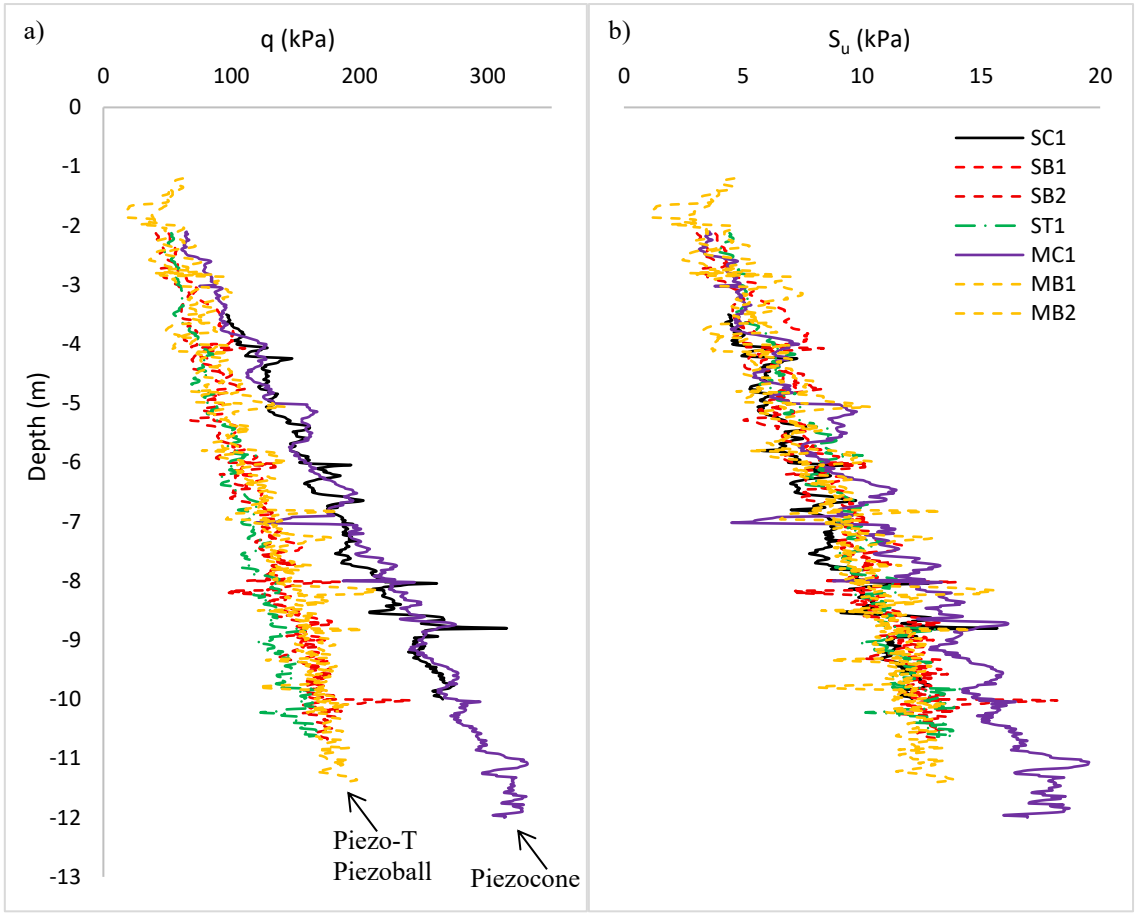
Figure 3.



The investigation program comprised seven field tests: two piezocone tests (SC1, MC1), four piezoball tests (SB1, SB2, MB1, MB2), and one piezo-T test (ST1). Figure 4 shows the cone resistance q_c (or q_m for full-flow) and undrained shear

strength S_u profiles, both recorded at 0.02 m intervals down to 10–13 m. The resistance profiles (Figure 4a) exhibit high mutual consistency, as do the S_u profiles (Figure 4b), confirming the representativeness of the database.

Figure 4.



As previously mentioned, an N_{kt} value of 15.5 was adopted to derive the undrained shear strength (S_u) from the piezocone tests, whereas N_b and N_t, bearing capacity factors for piezoball and piezo-T tests, respectively, of 13.0 and 11.8 were adopted. The calibration and characterisation of these bearing capacity factors are discussed in detail by Sosnoski et al. [51, 52]. The present study focuses on a different aspect, namely the assessment of local variability as a complementary tool for evaluating the applicability and reliability of piezo-T and piezoball tests in comparison with conventional piezocone

tests. Furthermore, the study aims to provide additional insights into the characterisation of local statistical descriptors relevant to geotechnical variability analyses.

Results and Discussions

Spatial correlation characterisation

The spatial variability of the lacustrine clay deposit was characterised via CPTu and penetrometer (piezoball and piezo-T) data from two independent campaigns: Sosnoski [30] and Meert [29]. Throughout the manuscript, CPTu and flow penetrometers sounding from Sosnoski [30] are designed as *S-series*, and those from Meert [29] are designed as *M-series*. The investigation campaign performed by Sosnoski [30] included one CPTu sounding (SC1), two piezoball tests (SB1 and SB2), and one piezo-T test (ST1). In contrast, the campaign conducted by Meert [29] involved one CPTu sounding (MC1) and two piezoball tests (MB1 and MB2). These identifiers are used throughout the paper when discussing and comparing the test results. Within each campaign, tests were performed in close proximity (≈ 1.5 m spacing) to enable direct comparisons between penetrometer types. The two investigation sites were approximately 50 m apart, ensuring that both campaigns sampled the same geological formation while providing independent datasets for assessing repeatability.

The field testing and data preprocessing procedures, including profile segmentation and stationarity verification, are described in the Methods section. The statistical parameters for all profiles, including the number of data points (ND), mean μ, standard deviation σ, coefficient of variation (COV), inherent COV (COV_w), and Kendall's tau p-values, are presented in Table 2.

Table 2. Statistical parameters and stationarity assessment for penetrometer profiles from the Tubarão/SC lacustrine clay deposit.

Test	Parameter	ND	μ (kPa)	σ (kPa)	COV	COVw	Kendall's τ	p-value	
SC1	q_c	326	183.24	51.53	0.28	0.06	0.057	0.13	Pass
	fs		4.77	1.45	0.30	0.14	-0.056	0.13	Pass
	u_2		131.86	41.85	0.32	0.05	-0.002	0.96	Pass
	S_u		8.39	2.44	0.29	0.09	0.047	0.21	Pass
SB1	q_m	354	114.48	35.01	0.31	0.07	-0.028	0.43	Pass
	u_1		200.60	81.26	0.41	0.05	0.004	0.91	Pass
	u_2		154.20	63.21	0.41	0.06	-0.032	0.37	Pass
	u_3		97.93	40.61	0.41	0.05	0.042	0.24	Pass
	S_u		8.60	2.62	0.30	0.08	-0.028	0.43	Pass
SB2	q_m	371	109.59	41.81	0.38	0.10	0.018	0.61	Pass
	u_1		211.15	89.67	0.42	0.06	-0.027	0.44	Pass
	u_2		155.23	64.42	0.41	0.08	-0.044	0.21	Pass
	u_3		99.37	40.36	0.41	0.06	-0.012	0.72	Pass
	S_u		8.21	3.14	0.38	0.10	0.018	0.60	Pass
ST1	q_m	299	103.23	33.38	0.32	0.07	-0.009	0.82	Pass
	S_u		8.59	2.77	0.32	0.07	-0.009	0.82	Pass
MC1	q_c	496	195.23	79.52	0.41	0.06	0.017	0.58	Pass
	fs		1.97	0.61	0.31	0.28	0.035	0.24	Pass
	u_2		131.18	62.90	0.48	0.07	0.015	0.61	Pass
	S_u		10.80	4.62	0.43	0.09	0.021	0.49	Pass
MB1	q_m	476	111.98	44.81	0.40	0.09	-0.003	0.93	Pass
	u_1		176.58	92.18	0.52	0.07	0.066	0.03	Fail
	u_2		91.14	53.32	0.59	0.10	0.153	0.00	Fail
	u_3		81.12	50.79	0.63	0.08	0.065	0.03	Fail
	S_u		7.89	3.12	0.40	0.10	-0.003	0.92	Pass
MB2	q_m	514	111.99	44.46	0.40	0.14	0.041	0.19	Pass
	u_1		159.89	94.33	0.59	0.15	0.052	0.10	Pass
	u_2		90.18	51.03	0.57	0.10	0.065	0.04	Fail
	u_3		82.43	42.05	0.51	0.09	0.087	0.01	Fail
	S_u		7.95	3.14	0.39	0.16	0.042	0.18	Pass

The vertical scale of fluctuation δ_v was estimated via the sample autocorrelation function (SAF) approach, with four TAMs (SNX, SQX, CSX, SMK) fitted to the

empirical data. Figure 5 illustrates the procedure for piezocone SC1 as a representative example.

Figure 5.

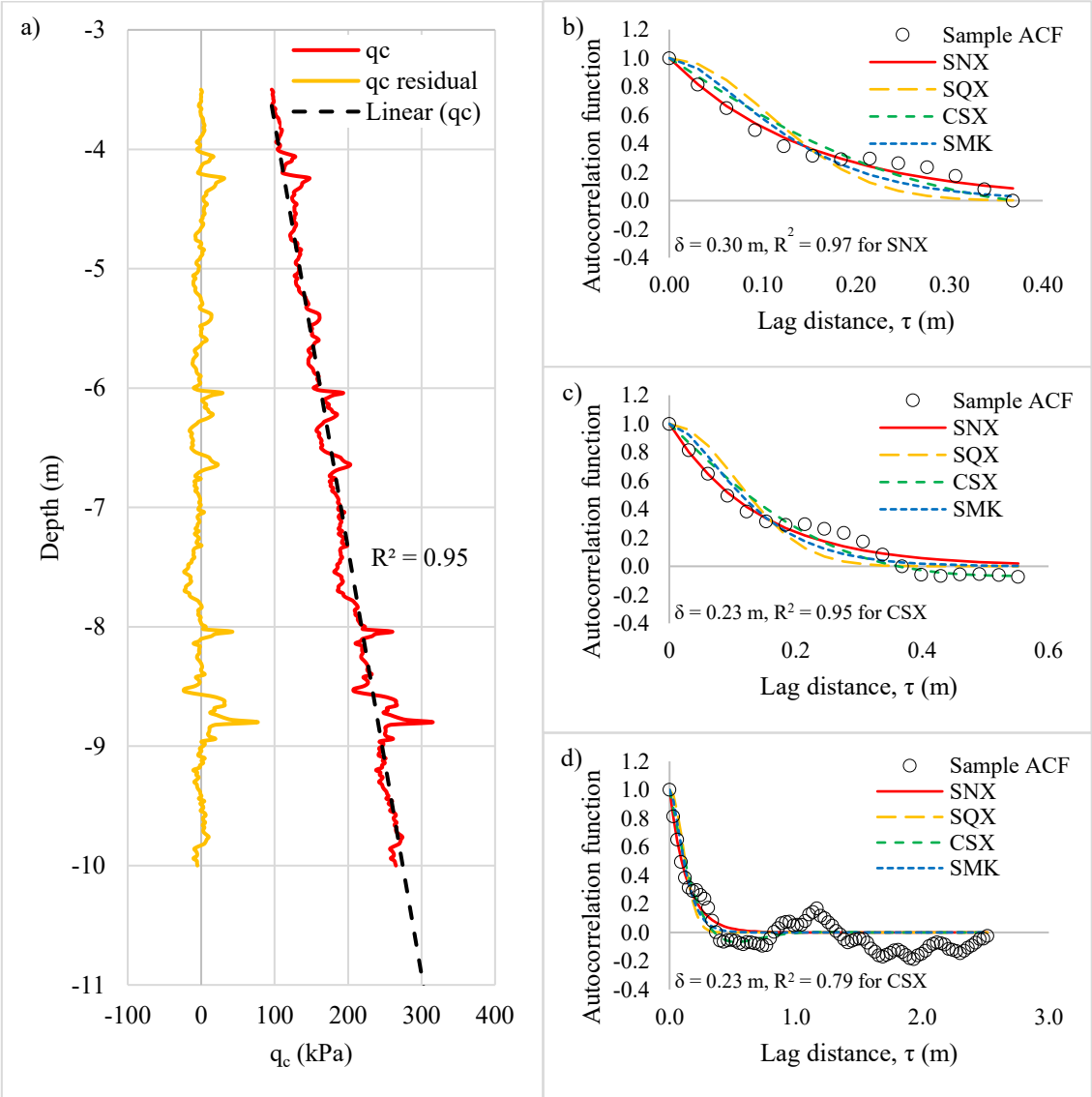


Figure 5a shows the original q_c profile and the fitted linear trend, which was removed to achieve stationarity (Kendall's p = 0.13). Figures 5b–5d present the SAF computed from the residuals, along with the best-fitting TAMs for each of the three criteria for maximum lag m. For $m = 12$ (Figure 5b), the best fit was the single exponential (SNX) model, yielding $\delta_v = 0.30$ m with $R^2 = 0.97$. For $m = \sqrt{n} +$

10 (Figure 5c, $m = 30$), the cosine exponential (CSX) model yields $\delta_v = 0.23$ m, $R^2 = 0.95$. For $m = n/4$ (Figure 5d), CSX again gave the best fit ($\delta_v = 0.23$ m, $R^2 = 0.79$).

Despite the substantial differences in lag distances among the three criteria, the estimated δ values remained largely consistent (0.30 m and 0.23 m), confirming the robustness of the estimation for this deposit. The higher R^2 values for fewer lags suggest that limiting the maximum lag improves the fit, which is consistent with recommendations to restrict analysis to the initial portion of the ACF [36, 46].

The results of the goodness-of-fit analysis for all profiles and TAMs are summarised in Table 3. For piezocone SC1, the SNX model with m = 12 gave the best fit for q_c (δ_v = 0.30 m, R^2 = 0.97), which is within the range reported for clayey deposits [1, 56]. For piezoball SB1 and SB2, the best fits were SNX with δ_v = 0.43 m (R^2 = 0.98) and SNX with δ_v = 0.15 m (R^2 = 0.99), respectively. For piezo-T ST1, CSX gave δ_v = 0.16 m (R^2 = 0.96). From the Meert [29] campaign, MC1 (piezocone) gave SNX with δ_v = 0.26 m (R^2 = 0.99), MB1 gave SNX with δ_v = 0.19 m (R^2 = 0.94), and MB2 gave SNX with δ_v = 0.28 m (R^2 = 1.00).

The δ values for S_u are practically identical to those for q_c and q_m, as expected from the linear proportionality. Notably, the SNX model with $m = 12$ provided the best fit for most profiles, with R^2 ranging from 0.94–1.00 for penetration resistance. These findings suggest that SNX is particularly suitable for describing the spatial correlation of this lacustrine clay, which is consistent with previous studies on fine-grained soils [49].

347 Table 3. Goodness-of-fit statistics for grouped datasets by penetrometer type.

		SNX			SQX			CSX			SMK		
Test	**Par.**	**m**	**δ (m)**	**R^2**	**m**	**δ (m)**	**R^2**	**m**	**δ (m)**	**R^2**	**m**	**δ (m)**	**R^2**
SC1	q_c	12	0.30	0.97	RT	0.27	0.85	RT	0.23	0.95	RT	0.27	0.92
	fs	RT	0.33	0.98	12	0.29	0.95	12	0.24	0.99	12	0.30	0.99
	u_2	12	0.09	0.97	12	0.07	0.90	12	0.08	0.90	12	0.08	0.94
	S_u	12	0.29	0.97	RT	0.26	0.86	RT	0.23	0.95	RT	0.27	0.93
SB1	q_m	12	0.43	0.98	RT	0.41	0.80	12	0.31	0.92	RT	0.43	0.91
	u_1	12	0.16	0.94	RT	0.13	0.80	RT	0.14	0.83	RT	0.14	0.86
	u_2	RT	0.28	0.92	RT	0.20	0.71	12	0.21	0.72	RT	0.24	0.80
	u_3	RT	0.13	0.96	RT	0.11	0.92	RT	0.09	0.88	RT	0.12	0.94
	S_u	12	0.43	0.98	RT	0.41	0.80	12	0.31	0.92	RT	0.43	0.91
SB2	q_m	12	0.15	0.99	12	0.15	0.94	12	0.12	0.97	12	0.15	0.98
	u_1	n/4	0.11	0.65	n/4	0.06	0.57	n/4	0.05	0.53	n/4	0.07	0.60
	u_2	12	0.12	0.87	12	0.09	0.72	12	0.08	0.68	12	0.10	0.79
	u_3	12	0.28	0.67	n/4	0.22	0.42	n/4	0.19	0.40	n/4	0.27	0.50
	S_u	12	0.15	0.99	12	0.15	0.94	12	0.12	0.97	12	0.15	0.98
ST1	q_m	12	0.19	0.92	12	0.19	0.86	12	0.16	0.96	12	0.19	0.90
	S_u	12	0.19	0.92	12	0.19	0.86	12	0.16	0.96	12	0.19	0.90
MC1	q_c	12	0.26	0.99	12	0.24	0.93	12	0.20	0.99	12	0.25	0.98
	fs	12	0.24	0.98	12	0.22	0.94	12	0.18	1.00	12	0.23	0.99
	u_2	12	0.31	0.99	12	0.27	0.70	12	0.23	0.92	12	0.28	0.88
	S_u	12	0.26	0.99	12	0.24	0.93	12	0.20	0.99	12	0.25	0.98
MB1	q_m	12	0.19	0.94	n/4	0.15	0.70	12	0.16	0.75	12	0.17	0.79
	u_1	RT	0.30	0.96	RT	0.27	0.76	RT	0.24	0.84	RT	0.28	0.86
	u_2	12	1.14	0.99	RT	0.76	0.96	12	0.66	1.00	RT	0.79	0.99
	u_3	12	1.05	1.00	RT	0.74	0.95	12	0.62	1.00	RT	0.76	0.99
	S_u	12	0.19	0.94	n/4	0.16	0.70	12	0.16	0.75	12	0.17	0.79
MB2	q_m	12	0.28	1.00	RT	0.25	0.87	12	0.21	0.96	12	0.26	0.93
	u_1	12	0.69	0.89	n/4	1.40	0.25	12	0.44	0.80	12	0.53	0.50
	u_2	RT	0.32	0.94	RT	0.31	0.77	RT	0.27	0.90	RT	0.31	0.86
	u_3	12	2.68	1.00	n/4	1.89	0.92	RT	1.48	1.00	n/4	1.90	0.96
	S_u	12	0.29	1.00	RT	0.25	0.87	12	0.21	0.96	12	0.26	0.93

348 *RT denotes the criterion m = √n + 10 (root); m = 12 and m = n/4 are the other criteria.

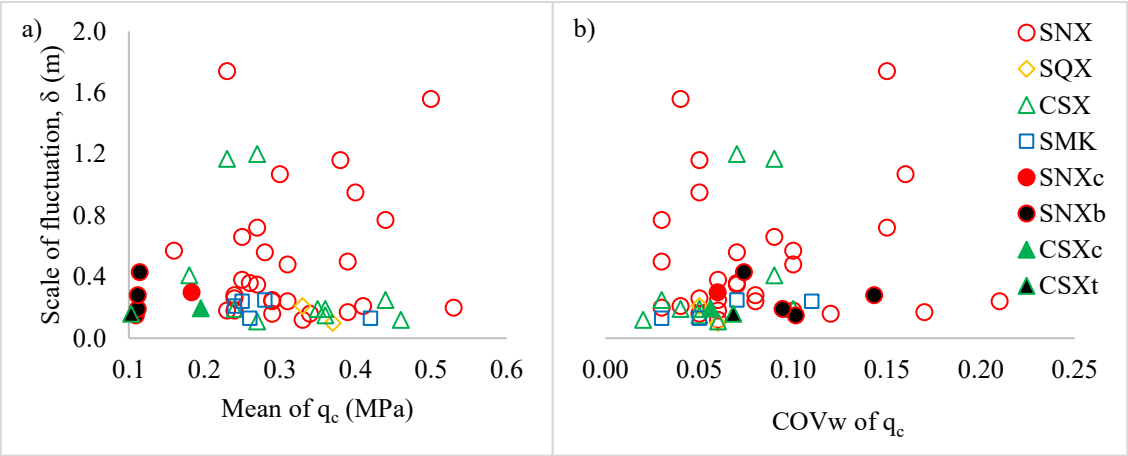
349

350 A comparison of the vertical δ values obtained in this study with those reported

351 by Lim and Lee [26] for Gwangyang marine clay is presented in Figure 6. The full-flow

penetrometers have lower mean resistances than the piezocone, as expected from the different soil-probe interaction mechanisms [14, 57]. However, when plotted against COV_w, the full-flow data integrate well with the piezocone results and the Lim and Lee [26] dataset. The COV_w values (0.05–0.10) fall within the range reported by the authors (0.02–0.21), confirming that the inherent variability of the lacustrine clay is consistent with that of other marine and lacustrine clays.

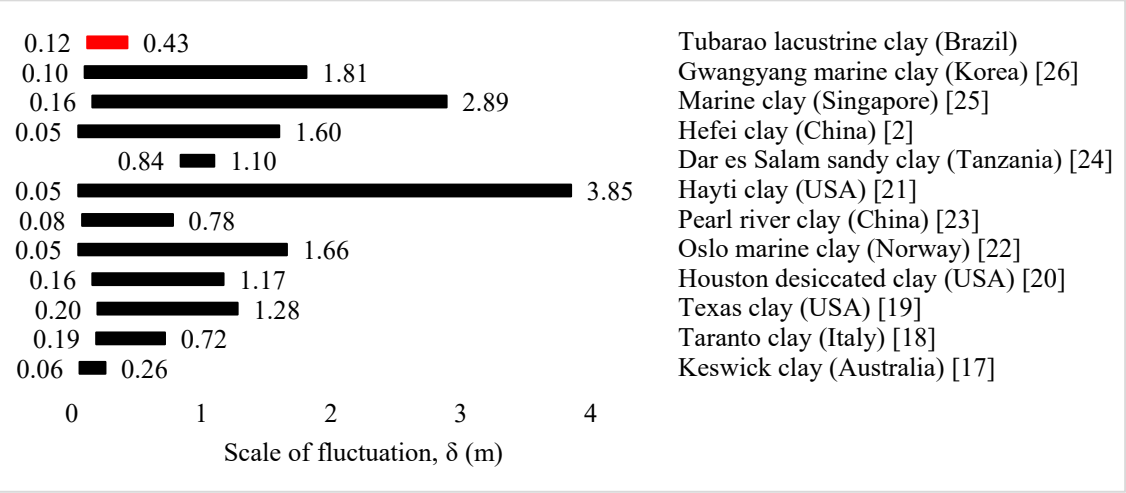
Figure 6.



The δ values from this study (0.12–0.43 m, based on penetration resistance) indicate moderate to high vertical spatial variability, characteristic of sedimentary deposits in low-energy environments [55].

A comparison of the δ range obtained in this study with those from other clay deposits worldwide is presented in Figure 7. The range obtained (0.12–0.43 m) lies in the lower portion of the ranges reported for Gwangyang (0.10–1.81 m), Oslo (0.05–1.66 m), and Hefei (0.16–2.89 m). This narrower range is likely due to the smaller number of tests (seven profiles from a single site) compared with larger databases (e.g., 51 profiles in Lim and Lee [26], 509 in Fei et al. [2], >200 in Jaksa [17]). Nevertheless, the consistency across different penetrometer types suggests that the estimated range is representative of the Tubarão deposit.

Figure 7.



Across all the TAMs, the mean δ ranged from 0.38 m (SMK) to 0.58 m (SNX), confirming that model choice can introduce variations of approximately 30%. Therefore, when selecting δ for reliability-based design, a range of values should be considered rather than a single deterministic estimate.

Design parameters

This section investigates the inherent variability of the undrained shear strength (S_u) of the Tubarão soft clay deposit for geotechnical design applications by evaluating theoretical probability density functions (PDFs) and determining the mean values and coefficients of variation (COVs) for each test type. For more representative site-specific characterisation, the in situ test profiles were grouped by penetrometer type: piezocone (SC1 + MC1), piezoball (SB1, SB2, MB1, MB2), and piezo-T (ST1, analysed separately). Table 4 presents the statistical parameters for each group, including the root mean square error (RMSE) and Pearson correlation coefficients obtained from the Q–Q plots.

Table 4. Goodness-of-fit statistics for grouped test datasets by penetrometer type.

	Piezocone		Piezoball		Piezo-T	
Parameter	**q_c**	**S_u**	**q_m**	**S_u**	**q_m**	**S_u**
μ (kPa)	190.48	9.84	111.98	8.13	103.23	8.59
σ (kPa)	70.07	4.08	42.15	3.04	33.43	2.78
COV	0.368	0.414	0.376	0.374	0.324	0.323
Pearson Normal	0.99	0.98	0.99	0.99	0.98	0.98
Pearson Lognormal	0.95	0.96	0.93	0.93	0.95	0.95
Pearson Gamma	0.98	0.98	0.97	0.97	0.97	0.97
Pearson Weibull	0.99	0.99	0.99	0.99	0.98	0.98
RMSE Normal	11.80	0.85	6.98	0.48	6.99	0.58
RMSE Lognormal	26.86	1.26	19.59	1.44	11.79	0.97
RMSE Gamma	16.33	0.74	11.51	0.83	8.44	0.70
RMSE Weibull	9.32	0.58	5.99	0.42	6.03	0.50

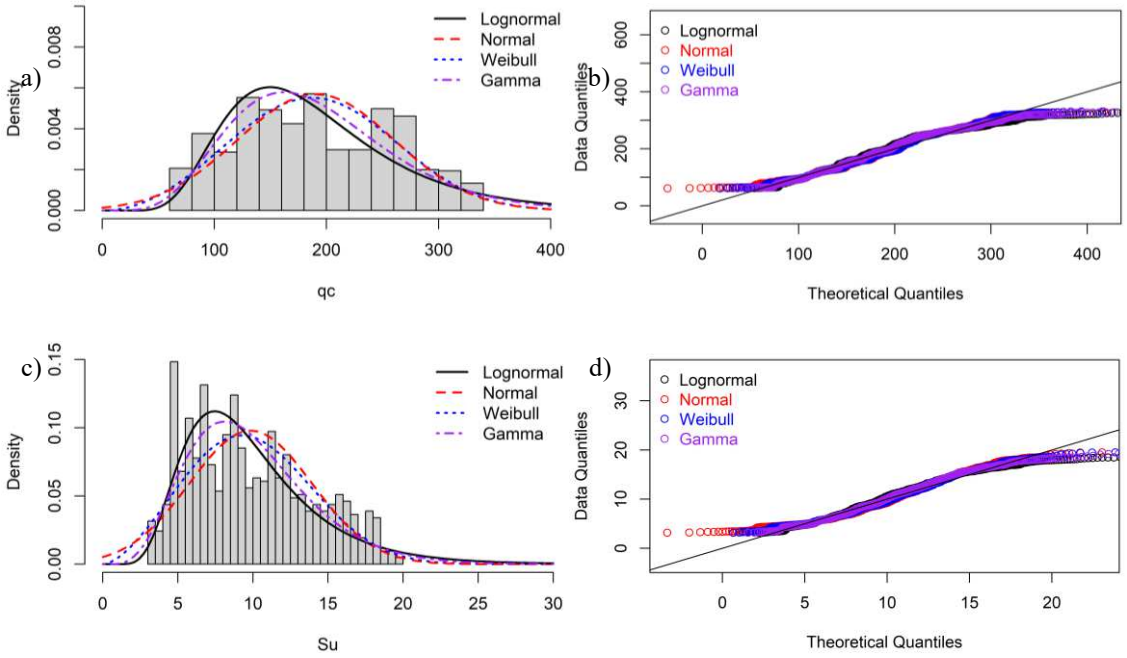
A preliminary examination of the results presented in Table 2 indicates differences in the mean undrained shear strength (S_u) of 17.4% and 12.7% for the piezoball and piezo-T tests, respectively, relative to the values obtained from the piezocone test. In addition to these differences in the mean values, the coefficients of variation (COVs) also reveal distinct levels of variability among the test methods. The piezocone results exhibit the highest variability, with a COV of 41.4%, compared with 37.4% for piezoball and 32.3% for piezo-T. Although these values differ slightly from those reported by Sosnoski et al. [51], they show the same overall trend of lower dispersion associated with full-flow penetrometers. These findings are consistent with the observations of DeJong et al. [14], who attributed the greater variability of S_u derived from CPTu tests to the greater sensitivity of the interpretation to the accuracy of penetration resistance and pore pressure measurements. In contrast, full-flow penetrometers exhibit a lower dependence on these factors, potentially providing more reliable estimates of undrained shear strength.

The goodness-of-fit of the four probability distributions was evaluated via Q-Q plots and quantitative error metrics (see Methods). These metrics were used to identify

407 the probability distribution that best fit the grouped data. The Weibull distribution
408 provided the highest correlation coefficients (0.98–0.99) for all the parameters, followed
409 by the normal (0.98–0.99), gamma (0.97–0.98), and lognormal (0.93–0.96). The root
410 mean square error (RMSE) analysis confirmed the superior fit of the Weibull distribution,
411 with the lowest RMSE values for both penetration resistance and S_u across all
412 penetrometer types (e.g., for piezocone q_c: Weibull RMSE = 9.32 kPa vs. normal 11.80
413 kPa). The Weibull flexibility in capturing the skewness typical of penetration resistance
414 data explains its better performance, which is consistent with Tigabu Abera and Kirianova
415 [58]. Nevertheless, the normal distribution also provides a reasonable approximation
416 (correlation coefficients > 0.98 and RMSE close to the Weibull), making it a viable option
417 for practical applications where simplicity is preferred [1].
418 Histograms and Q-Q plots for the grouped datasets (piezocone, piezoball, and
419 piezo-T) are presented in Figures 8, 9, and 10, respectively. The histograms for
420 penetration resistance and for S_u show right-skewed distributions, which are typical of
421 soft clay measurements. The Q-Q plots confirm that the Weibull distribution provides the
422 closest match to the 1:1 reference line, followed by the normal and gamma distributions;
423 the lognormal distribution shows the largest deviations, especially at the tails. This visual
424 assessment corroborates the quantitative goodness-of-fit results.
425 Figure 11 presents the probability density functions (PDFs) of the best-fitting
426 Weibull distributions for each penetrometer type. For penetration resistance (Figure 6a),
427 the piezocone PDF (black) is shifted to the right (mean 190.48 kPa), reflecting the higher
428 resistance mobilised by the conical tip due to cavity expansion [14, 57].
429 The piezoball and piezo-T PDFs have lower means (111.98 and 103.23 kPa,
430 respectively), with the piezo-T PDFs showing the narrowest distribution. In contrast, the
431 PDFs for S_u (Figure 6b) converge remarkably well across the three penetrometer types

(i.e., piezocone 9.84 kPa, piezoball 8.13 kPa, and piezo-T 8.59 kPa). This convergence demonstrates the effectiveness of the site-specific bearing capacity factors ($N_{kt} = 15.5, N_b = 13.0, N_t = 11.8$) in normalising the penetration resistance to a consistent estimate of the undrained shear strength. Furthermore, the full-flow penetrometers exhibit narrower probability distributions than the piezocone does, indicating lower data dispersion. This observation is consistent with the lower coefficients of variation reported in Table 2 and reinforces the robustness of the characterisation, as well as the applicability of full-flow penetrometers for soft soil investigations, in agreement with previous studies [14, 16, 59].

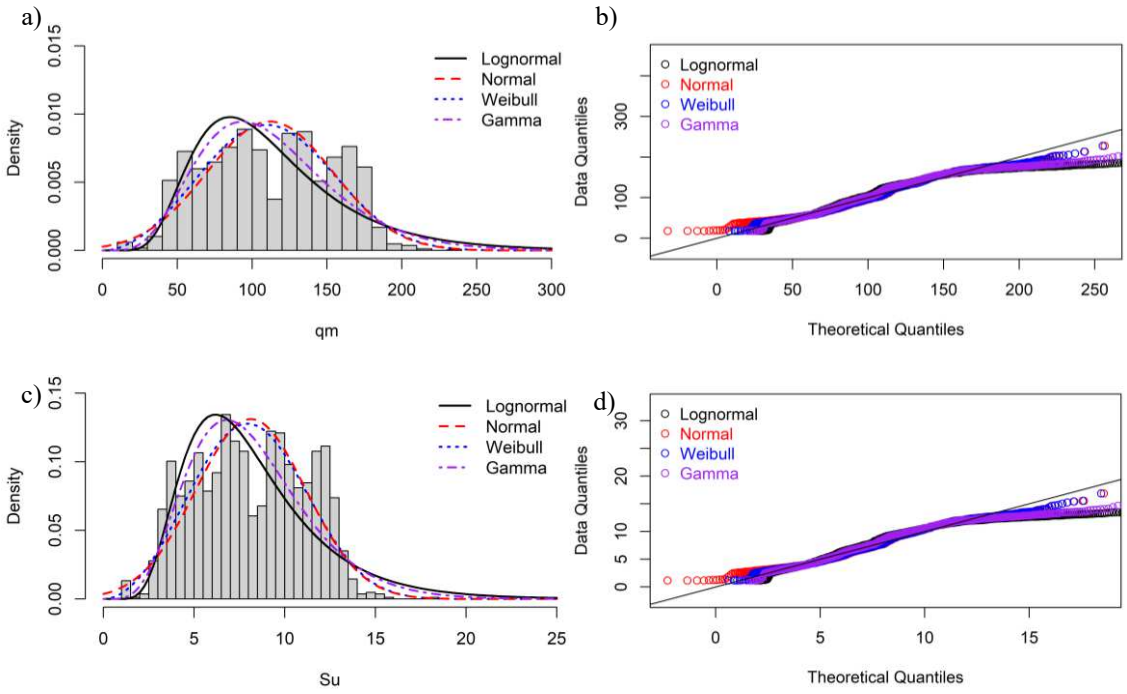
Figure 8.



The spatial correlation characterisation and design parameter analysis presented here provide a useful framework for assessing the spatial variability and geotechnical properties of lacustrine clay deposits. The results demonstrate the effectiveness of CPT-based methods for spatial variability characterisation and highlight the importance of incorporating spatial correlation in geotechnical design. The derived statistical

449 parameters and δ estimates can serve as inputs for stochastic analyses, contributing to
450 more reliable foundation designs under similar soil conditions.

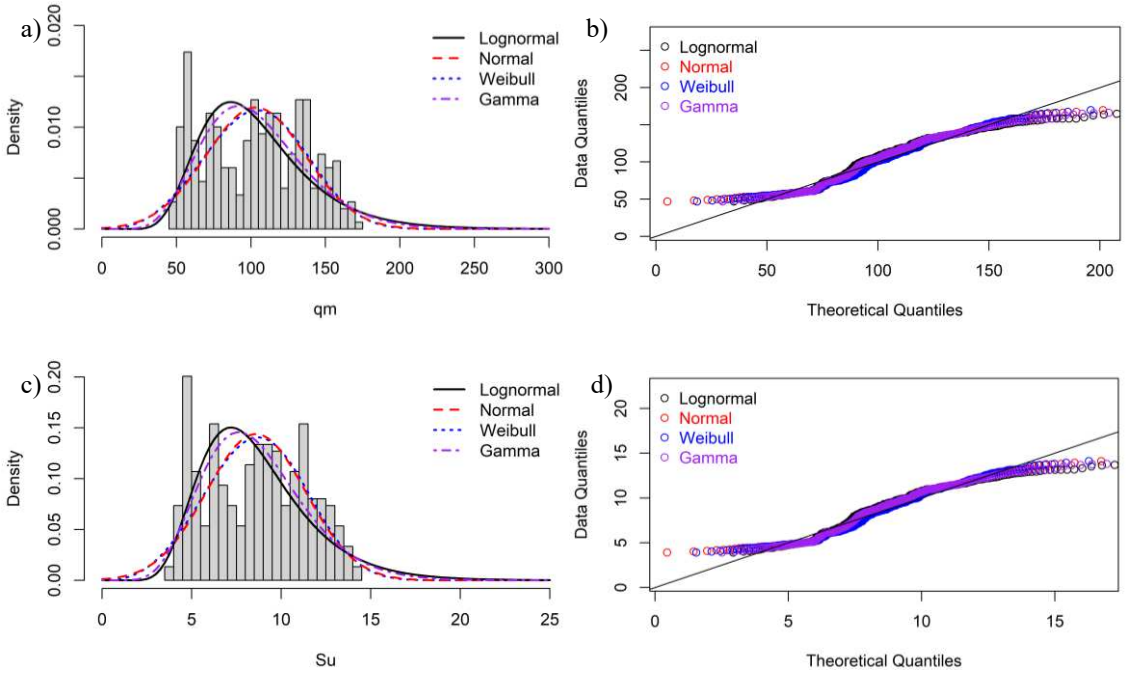
451 Figure 9.



452

453

454 Figure 10.

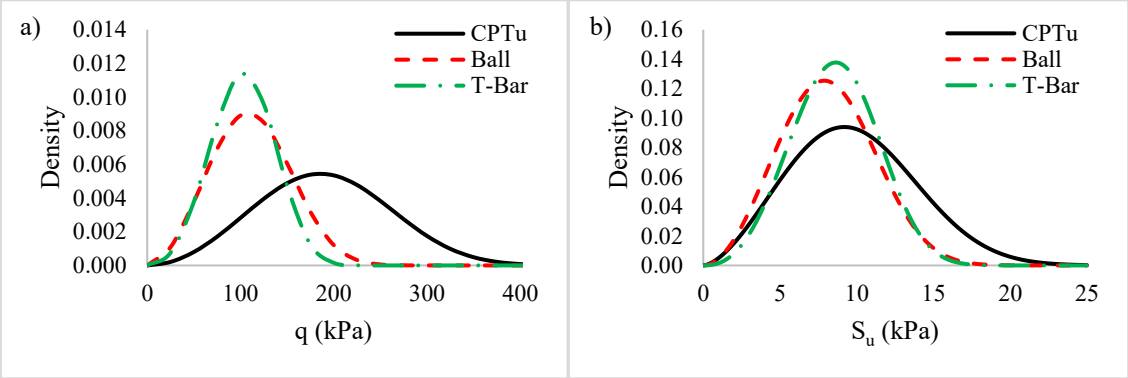


455

456

457

458 Figure 11.



459

460 **Conclusions**

461 This study provides a direct quantitative comparison between conventional piezocone
462 (CPTu) tests and full-flow penetrometers, namely, piezoball and piezo-T. This study
463 complements the characterisation of a Brazilian soft clay deposit previously presented by
464 Sosnoski et al. [51, 52] and extends those investigations through a comprehensive
465 assessment of the applicability of full-flow penetrometers for spatial variability analyses.
466 While the study is novel in that it introduces piezoball testing into Brazilian geotechnical
467 practice, it also contributes to broader international efforts to evaluate and consolidate the
468 use of these devices.

469 This study emphasises a rigorous characterisation of sounding profiles through
470 trend removal and verification of stationarity prior to spatial variability analyses. It further
471 investigates the influence of both the number of lags and the selected theoretical
472 autocorrelation model (TAM) on the estimation of the vertical scale of fluctuation. In
473 addition, the inherent variability of the undrained shear strength is evaluated as a key
474 parameter for geotechnical design. On the basis of the presented results, the following
475 conclusions can be drawn:

476 Despite the limited experimental dataset (only seven soundings), the test program
477 proved adequate for the characterisation of local spatial variability within the Tubarão

deposit. While the quantitative findings are considered representative for this specific site, caution is advised when extrapolating the derived statistical parameters to other geological contexts without complementary site-specific investigations. Future investigations should therefore be expanded and complemented with additional characterisation techniques, such as seismic, pressuremeter, and sampling-based investigations, to further improve the robustness of the statistical characterisation.

Although the analysed deposit exhibited a relatively homogeneous soil profile, the proposed behaviour-based profile segmentation proved to be a robust preprocessing strategy for variability characterisation. However, profile segmentation should always be complemented by stationarity verification (e.g., Kendall's tau test) to ensure that the analysed segments satisfy the assumptions required for random field characterisation. Therefore, careful preprocessing of in situ test data remains a fundamental step in spatial variability analyses.

With respect to the theoretical autocorrelation models (TAMs), the SNX model generally provided the best fit to the experimental autocorrelation functions. Nevertheless, noticeable differences were observed among the estimated scales of fluctuation obtained with the various TAMs. Therefore, careful evaluation of the adopted autocorrelation model is recommended, as model selection may significantly influence the derived spatial variability descriptors and, consequently, subsequent random field analyses.

The combined evaluation of probability density functions (PDFs) and basic statistical descriptors (mean, standard deviation, and coefficient of variation) demonstrated that the piezoball and piezo-T tests provide results that are consistent with those obtained from conventional CPTu soundings. In addition, the full-flow penetrometers generally exhibited lower data dispersion, suggesting their potential

applicability for geotechnical characterisation and for applications requiring estimates of local variability, such as probabilistic analyses and random field modelling.

Acknowledgements

The authors gratefully acknowledge the financial support provided by FAPESC (Foundation for Research and Innovation of the State of Santa Catarina) and CAPES (Coordination for the Improvement of Higher Education Personnel). Thanks are also extended to the Postgraduate Program in Civil Engineering (PPGEC) at the Federal University of Santa Catarina for the institutional support and infrastructure provided throughout this investigation. The authors gratefully acknowledge the Federal University of Technology – Paraná (UTFPR) for granting a period of academic leave.

Author contributions

A.L.M. wrote the main manuscript text and performed the spatial variability analyses. G.D. supervised the research, contributed to the statistical analysis, and reviewed the manuscript. M.A.F. contributed to the writing and revision of the article. J.S. conducted the field tests and provided the database. All the authors reviewed and approved the final manuscript.

Data availability statement

The datasets generated and/or analysed during the current study are available from the corresponding author upon reasonable request.

Competing interests

No potential conflicts of interest were reported by the authors.

Funding

This study was financed in part by the Coordination for the Improvement of Higher Education Personnel – Brazil (CAPES) and the Foundation for Research and Innovation of the State of Santa Catarina (FAPESC).

Declaration of generative AI use

The authors report that generative AI was not used in their research or preparation of this manuscript.

References

[1] Phoon, K. K. & Kulhawy, F. H. Characterization of geotechnical variability. *Can. Geotech. J.* 36, 612-624 (1999).

[2] Fei, S. et al. Evaluation of the scale of fluctuation based on variance reduction method. *Eng. Geol.* **308**, 106804 (2022).

[3] Salgado, R., Prezzi, M. & Ganju, E. Assessment of site variability from analysis of cone penetration test data. *Joint Transp. Res. Program Publ. No. FHWA/IN/JTRP-2015/04*, Purdue Univ. (2015).

[4] Teh, C. I. & Houlsby, G. T. An analytical study of the cone penetration test in clay. *Géotechnique* **41**, 17-34 (1991).

[5] Su, S. F. & Liao, H. J. Influence of strength anisotropy on piezocone resistance in clay. *J. Geotech. Geoenviron. Eng.* **128**, 166-173 (2002).

[6] Mayne, P. W. *Cone Penetration Testing: A Synthesis of Highway Practice*. NCHRP Synthesis 368, Transp. Res. Board, Washington, D.C. (2007).

[7] Robertson, P. K. Interpretation of cone penetration tests – A unified approach. *Can. Geotech. J.* **46**, 1337-1355 (2009).

[8] Schnaid, F. *In Situ Testing in Geomechanics: The Main Tests*. Taylor & Francis Group, London (2009).

[9] Low, H. E. et al. Estimation of intact and remoulded undrained shear strengths from penetration tests in soft clays. *Géotechnique* **60**, 843-859 (2010).

[10] Basarah, Y. I. et al. Interpreting the undrained shear strength of soft clays using CPTu: evaluation of cone bearing factor (Nkt) and related practical soil parameters at selected sites in Western Java. *Geotechnics* **6**, 1-23 (2026).

[11] Chen, X., Han, C., Liu, J. & Hu, Y. Interpreting strength parameters of strain-softening clay from shallow to deep embedment using ball and T-bar penetrometers. *Comput. Geotech.* **138**, 104331 (2021).

[12] Colreavy, C., O'Loughlin, C. D., Long, M., Boylan, N. & Ward, D. Field experience of the piezoball in soft clay. In *Proc. 2nd Int. Symp. Cone Penetration Test. (CPT'12)*, 111-118, Huntington Beach, CA (2012).

[13] Mahmoodzadeh, H., Wang, D. & Randolph, M. F. Interpretation of piezoball dissipation testing in clay. *Géotechnique* **65**, 831-842 (2015).

[14] DeJong, J. T., Yafrate, N. J. & DeGroot, D. J. Evaluation of undrained shear strength using full-flow penetrometers. *J. Geotech. Geoenviron. Eng.* **137**, 14-26 (2011).

[15] O'Loughlin, C., White, D., Randolph, M. F., Zhou, Z. & Stanier, S. Advances in full flow penetrometer testing. In *6th Int. Conf. Geotech. Geophys. Site Charact.*, 1-8, ISSMGE (2020).

[16] Qiao, H. et al. The practice and development of T-bar penetrometer tests in offshore engineering investigation: a comprehensive review. *J. Mar. Sci. Eng.* **11**, 1160 (2023).

[17] Jaksa, M. B. *The influence of spatial variability on the geotechnical design properties of a stiff, overconsolidated clay*. Ph.D. thesis, Univ. Adelaide, Australia (1995).

[18] Cafaro, F. & Cherubini, C. Large sample spacing in evaluation of vertical strength variability of clayey soil. *J. Geotech. Geoenviron. Eng.* **128**, 558-568 (2002).

[19] Akkaya, A. D. & Vanmarcke, E. H. Estimation of spatial correlation of soil parameters based on data from the Texas A&M University NGES. In *Probabilistic Site Charact. at the National Geotech. Experimentation Sites (GSP 121)*, 29-40, ASCE, Reston, VA (2003).

[20] Stuedlein, A. W., Kramer, S. L., Arduino, P. & Holtz, R. D. Geotechnical characterization and random field modeling of desiccated clay. *J. Geotech. Geoenviron. Eng.* **138**, 1301-1313 (2012).

[21] Onyejekwe, S., Kang, X. & Ge, L. Evaluation of the scale of fluctuation of geotechnical parameters by autocorrelation function and semivariogram function. *Eng. Geol.* **214**, 43-49 (2016).

[22] Liu, Z., Lacasse, S., Nadim, F., Vanneste, M. & Yetginer, G. Accounting for the spatial variability of soil properties in the reliability-based design of offshore piles. In *Front. Offshore Geotech. III – Proc. 3rd Int. Symp. Front. Offshore Geotech. (ISFOG 2015)*, Vol. 1, 1375-1380, London (2015).

[23] Bombasaro, E. & Kasper, T. Evaluation of spatial soil variability in the Pearl River Estuary using CPTU data. *Soils Found.* **56**, 496-505 (2016).

[24] Lingwanda, M. I., Prastings, A., Larsson, S. & Nyaoro, D. L. Comparison of geotechnical uncertainties linked to different soil characterization methods. *Geomech. Geoeng.* **12**, 137-151 (2017).

[25] Wang, Z. Z., Guo, X. & Hu, Y. Characterisation of the spatial variability of underconsolidated Singapore marine clay using random field theory. *Georisk* **19**, 448-466 (2025).

595 [26] Lim, C. H. & Lee, J. K. CPT-based spatial variability of marine clay: a case study
596 from Gwangyang Bay of Korea. *Ocean Eng.* **354**, 124810 (2026).
597 [27] Fenton, G. A. Random field modeling of CPT data. *J. Geotech. Geoenviron.*
598 *Eng.* **125**, 486-498 (1999).
599 [28] Macedo, J. et al. CPTu-based spatial variability assessment of thickened and
600 conventional mine tailings. *J. Geotech. Geoenviron. Eng.* **150**, 04024091 (2024).
601 [29] Meert, R. L. B. *Desenvolvimento, Execução e Validação dos Ensaios de Barra e*
602 *Bola*. Master's thesis, Univ. Estado de Santa Catarina, Joinville, Brazil (2022).
603 [30] Sosnoski, J. *Caracterização de Solos Moles Através de Penetrômetros de Fluxo*.
604 Ph.D. thesis, Univ. Federal de Santa Catarina, Florianópolis, Brazil (2024).
605 [31] Fenton, G. A. & Griffiths, D. V. *Risk Assessment in Geotechnical Engineering*. John
606 Wiley & Sons, New York (2008).
607 [32] Vanmarcke, E. H. Probabilistic modeling of soil profiles. *J. Geotech. Eng. Div.,*
608 *ASCE* **103**, 1227-1246 (1977).
609 [33] Phoon, K. K., Kulhawy, F. H. & Grigoriu, M. D. *Reliability-Based Design of*
610 *Foundations for Transmission Line Structures*. Rep. TR-105000, Electr. Power Res. Inst.,
611 Palo Alto, CA (1995).
612 [34] Uzielli, M., Vannucchi, G. & Phoon, K. K. Random field characterisation of stress-
613 normalised cone penetration testing parameters. *Géotechnique* **55**, 3-20 (2005).
614 [35] Phoon, K. K., Quek, S. T. & An, P. Identification of statistically homogeneous soil
615 layers using modified Bartlett statistics. *J. Geotech. Geoenviron. Eng.* **129**, 649-659
616 (2003).
617 [36] Jaksa, M. B., Brooker, P. I. & Kaggwa, W. S. Inaccuracies associated with estimating
618 random measurement errors. *J. Geotech. Geoenviron. Eng.* **123**, 393-401 (1997).
619 [37] DeGroot, D. J. & Baecher, G. B. Estimating autocovariance of in-situ soil
620 properties. *J. Geotech. Eng.* **119**, 147-166 (1993).
621 [38] Jaksa, M. B., Kaggwa, W. S. & Brooker, P. I. Experimental evaluation of the scale
622 of fluctuation of a stiff clay. In *Proc. 8th Int. Conf. Appl. Stat. Probab.*, Vol. 1, 415-422,
623 Sydney (1999).
624 [39] ASTM D5778-2020. *Standard Test Method for Electronic Friction Cone and*
625 *Piezocone Penetration Testing of Soils*. ASTM Int. (2020).
626 [40] NBR 12069:1991. *Ensaio de Penetração de Cone In Situ (CPT) – Método de Ensaio*.
627 ABNT (1991).

628 [41] ISO 19901-8:2014. *Petroleum and Natural Gas Industries – Specific Requirements*
629 *for Offshore Structures – Part 8: Marine Soil Investigations*. ISO (2014).
630 [42] Robertson, P. K. & Wride, C. E. Evaluating cyclic liquefaction potential using the
631 cone penetration test. *Can. Geotech. J.* **35**, 442-459 (1998).
632 [43] Bowerman, B. L. & O'Connell, R. T. *Forecasting and Time Series*. Duxbury Press,
633 Massachusetts (1979).
634 [44] Brockwell, P. J. & Davis, R. A. *Time Series: Theory and Methods*. Springer-Verlag,
635 New York (1987).
636 [45] Hyndman, R. J. *PEST – A Program for Time Series Analysis*. Stat. Consult. Centre,
637 Univ. Melbourne, Australia (1990).
638 [46] Box, G. E. P., Jenkins, G. M. & Reinsel, G. C. *Time Series Analysis: Forecasting*
639 *and Control*. 3rd ed., Prentice Hall, New Jersey (1994).
640 [47] Dasaka, S. M. & Zhang, L. M. Spatial variability of in situ weathered
641 soil. *Géotechnique* **62**, 375-384 (2012).
642 [48] Cryer, J. D. *Time Series Analysis*. Duxbury Press, Boston (1986).
643 [49] Bong, T. & Stuedlein, A. W. Spatial variability of CPT parameters and silty fines in
644 liquefiable beach sands. *J. Geotech. Geoenviron. Eng.* **143**, 04017093 (2017).
645 [50] Davis, J. C. *Statistics and Data Analysis in Geology*. 2nd ed., John Wiley & Sons,
646 New York (1986).
647 [51] Sosnoski, J. et al. Performance of piezoball and piezo-T flow penetrometers
648 compared with conventional in situ tests in Brazilian soft soils. *Geotechnics* **6**, 24
649 (2026a).
650 [52] Sosnoski, J., Dienstmann, G., Meier, A. L., Odebrecht, E. & Nierwinski, H. P.
651 Undrained shear strength degradation and consolidation coefficients evaluation
652 considering a piezoball penetrometer: application on a Brazilian soft soil deposit. *Soils*
653 *Rocks* **49**, e2026008625 (2026b).
654 [53] Mantaras, F. M., Odebrecht, E. & Schnaid, F. Using piezocone dissipation test to
655 estimate the undrained shear strength in cohesive soil. *Can. Geotech. J.* **52**, 318-325
656 (2015).
657 [54] Schnaid, F., Odebrecht, E., Sosnoski, J. & Robertson, P. K. Effects of test procedure
658 on flat dilatometer test (DMT) results in intermediate soils. *Can. Geotech. J.* **53**, 1270-
659 1280 (2016).

660 [55] Odebrecht, E. & Schnaid, F. Assessment of the stress history of Quaternary clay
661 from piezocone tests. *Soils Rocks* **41**, 179-189 (2018).
662 [56] Cami, B., Javankhoshdel, S., Phoon, K. K. & Ching, J. Scale of fluctuation for
663 spatially varying soils: estimation methods and values. *ASCE-ASME J. Risk Uncertain.*
664 *Eng. Syst. A Civ. Eng.* **6**, 03120002 (2020).
665 [57] Lunne, T., Andersen, K. H., Low, H. E., Randolph, M. F. & Sjursen, M. Guidelines
666 for offshore in situ testing and interpretation in deepwater soft clays. *Can. Geotech. J.* **48**,
667 543-556 (2011).
668 [58] Tigabu Abera, N. & Kirianova, L. Assessment of the distribution of the soil
669 deformation modulus based on CPT data. *Int. J. Comput. Civ. Struct. Eng.* **21**, 171-176
670 (2025).
671 [59] Yafrate, N. J., DeJong, J. T., DeGroot, D. J. & Randolph, M. F. Evaluation of
672 remolded shear strength and sensitivity of soft clay using full-flow penetrometers. *J.*
673 *Geotech. Geoenviron. Eng.* **135**, 1179-1189 (2009).

674 **Figure Legends**

675 Figure 1. Piezoball (spherical) and piezo-T (cylindrical T-bar) probes were used for full-
676 flow penetration testing (Meert, 2022).
677 Figure 2. Locations of the geotechnical investigation campaigns at the Tubarão Testing
678 Site.
679 Figure 3. Representative stratigraphic profile: (a) corrected cone resistance q_t and pore
680 pressure u_2, (b) soil behaviour index $I_{C,RW}$, and (c) undrained shear strength S_u (Sosnoski,
681 2024).
682 Figure 4. Geotechnical profiles: (a) penetration resistance (q), and (b) undrained shear
683 strength (S_u).
684 Figure 5. Vertical scale of fluctuation estimation procedure for piezocone profile SC1. (a)
685 Original qc profile with a fitted linear trend; (b) SAF and TAMs for m = 12; (c) SAF and
686 TAMs for m = √n + 10; (d) SAF and TAMs for m = n/4.
687 Figure 6. Comparison of vertical δ values with data from Lim and Lee (2026) for
688 Gwangyang marine clay. (a) δ as a function of mean penetration resistance; (b) δ as a
689 function of inherent coefficient of variation (COVw).
690 Figure 7. Comparison of vertical scale of fluctuation (δ) ranges for clay deposits
691 worldwide.

692 Figure 8. Histograms and Q-Q plots for the piezocone grouped dataset. (a) Histogram of
693 q_c; (b) Q-Q plot of q_c; (c) Histogram of S_u; (d) Q-Q plot of S_u.
694 Figure 9. Histograms and Q-Q plots for the piezoball grouped dataset. (a) Histogram of
695 q_c; (b) Q-Q plot of q_c; (c) Histogram of S_u; (d) Q-Q plot of S_u.
696 Figure 10. Histograms and Q-Q plots for the piezo-T grouped dataset. (a) Histogram of
697 q_c; (b) Q-Q plot of q_c; (c) Histogram of S_u; (d) Q-Q plot of S_u.
698 Figure 11. Probability density functions (PDFs) of the best-fitting Weibull distributions
699 for each penetrometer type. (a) Penetration resistance (q_c for piezocone, q_m for piezoball
700 and piezo-T); (b) Undrained shear strength (S_u).